Progress In Electromagnetics Research M, Vol. 39, 19–26, 2014

Estimation of Whole-Body Average SAR in Human Body Exposed to a Base Station Antenna

Md. F. Ali[1, *] and Sudhabindu Ray[2]

Abstract—Electromagnetic wave absorption inside a human body is investigated. The human body has been modeled using 3D voxel based dataset considering different electrical parameters. At GSM 900 band, Specific Absorption Rate (SAR) induced inside the human body model exposed to a radiating base station antenna (BSA) has been calculated for multiple number of carrier frequencies and input power of 20 W/carrier. Distance (R) of human body from BSA is varied in the range of 0.5 m to 5.0 m. Values of whole-body average SAR obtained by hybrid FDTD method closely match with that obtained by SFDTD method. For number of carrier frequency equal to five and $R = 0.5$ m, maximum value of whole-body average SAR obtained by both hybrid FDTD and SFDTD method is found to be 0.69 W/kg which decreases either with increase of R or decrease of number of carrier frequencies. Safety distance for general public is found to be 1.5 m for number of carrier frequencies equal to five. Summary of performance comparison shows that hybrid FDTD method is faster and requires less memory than SFDTD method.

1. INTRODUCTION

Modern mobile telecommunication is based on the cellular system. In a cellular system the covering area is divided into a number of cells. Frequency band allocated to a cellular system for an operator is distributed over a group of cells and this distribution is repeated over the total service area. Each cell is covered by an allocated base station which keeps track of the mobile phones within its range, connects them to the telephone network and handles carry-over to the next base station when a customer is leaving the coverage area [1]. The radii of cells may vary in size according to the desired capacity and geographical area to be covered [2]. But now-a-days, with the introduction of digital mobile phone systems, cell sizes got much smaller and base stations are erected in close of houses, schools etc., in densely populated areas.

When electromagnetic (EM) waves radiated from the transmitting mobile telephone base station antenna (BSA) directly pass through human body, a significant portion of the radiated power is absorbed by the body tissues [3]. Human body is non-homogeneous and anisotropic in nature. Absorption of EM waves at radiofrequency (RF) inside human body creates standing waves, which causes localized hot spots [4]. The energy absorptions due to localized hot spots may result in boils, drying up the fluids around eyes, brain, joints, heart, abdomen, etc.. Higher level of non ionizing radiation may damage DNA of the living tissues [5–7]. Large number of investigations on the hazardous effects of mobile telephone BSAs are available in the literature but very few of that are available on the effects on wellbeing [8]. The current international safety guidelines or standards have been established for avoiding or limiting the potentially hazardous exposures of human head and other body parts from the adverse biological effects due to RF exposure [9, 10].

Received 2 August 2014, Accepted 15 September 2014, Scheduled 25 September 2014

* Corresponding author: Md. Faruk Ali (faruk_ali@rediffmail.com).

[1] Department of Electronics and Instrumentation Engineering, Nazrul Centenary Polytechnic, West Bengal, Burdwan 713335, India.

[2] Department of Electronics and Telecommunication Engineering, Jadavpur University, West Bengal, Kolkata 700032, India.

An attempt has been made to estimate Specific Absorption Rate (SAR) and total absorbed power for whole-body, partial-body and localized exposure inside a simple box-shaped phantom placed in close vicinity of a typical representative base station panel antenna [11, 12]. In this study, whole-body average SAR (SAR_{WB}) induced within the full human body model exposed to a BSA at GSM 900 band for a distance (R) in the range of 0.5 m to 5.0 m between the human body and the BSA has been calculated using Hybrid Finite Difference in Time Domain (Hybrid FDTD) method and compared that with the results obtained by Segmented Finite Difference in Time Domain (SFDTD) method for multiple number of carrier frequencies [13]. To solve large scale problems, both the hybrid FDTD and SFDTD methods are used to reduce the computational requirements and enhances the practicability of running the simulation on a PC. But this study shows that hybrid FDTD method is faster and requires less memory than SFDTD method. Computer code of hybrid FDTD and SFDTD methods have been developed using the MATLAB software [14].

2. SYSTEM MODEL

2.1. Human Body Model

The full human body model has been constructed from voxel based Zubal phantom which is based on CT scan data of a 35 year old physically normal male weighing 70.31 kg and measuring 1.78 m in height [15]. MATLAB program is used to read, resample and reshape the phantom volume data consists of $192 \times 96 \times 498$ voxels, each having dimensions of 3.6 mm $\times$ 3.6 mm $\times$ 3.6 mm. To simplify the numerical calculations, resolution of the human body is reduced to $75 \times 75 \times 245$ voxels, each of dimensions: 5.0 mm $\times$ 5.0 mm $\times$ 5.0 mm. Geometry of the human body model along with BSA is shown in Fig. 1. The human body is comprised of eighty seven types of tissues. Mass density (ρ), relative dielectric constant (ε_r) and conductivity (σ) of different tissues at GSM 900 band are obtained from the literature [16].

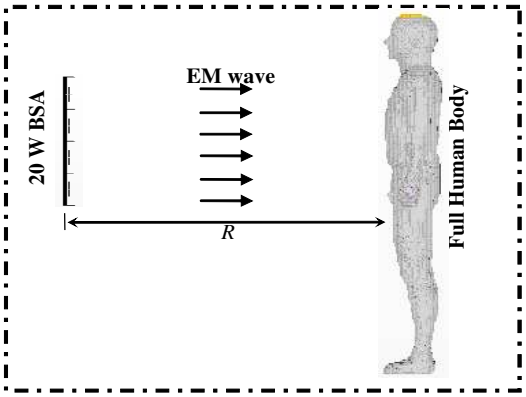

Figure 1. Geometry of BSA along with the human body model.

2.2. Base Station Antenna Model

The BSA used in the simulation is representative for the "Eurocell Panels" family of BSAs for vertical polarization offered by Kathrein in the frequency range from 870 MHz to 960 MHz. Geometry of the antenna model is reasonably close to that of the K730370 antenna and available in the literature [11, 12]. Transmitted power from BSA is equal to 20 W/carrier.

2.3. SFDTD Method

For large problem space, SFDTD method is used which divides the main space into different segments to reduce the computational requirements and enhances the practicability of running the simulation

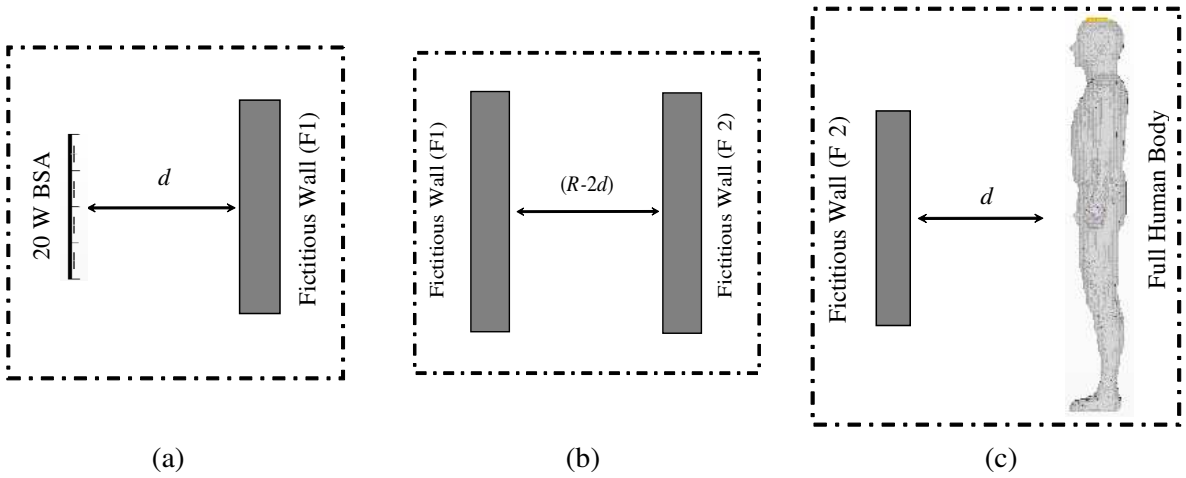

Figure 2. Geometry of the (a) antenna segment, (b) intermediate segment and (c) body segment.

on a PC [13]. For that reason in this study, SFDTD method has been used to carry out the required numerical evaluation of SAR and EM field distributions inside human body model. The actual space is split into three different 3-dimensional segments: antenna segment, intermediate segment and body segment as shown in the Figs. 2(a)–(c). In SFDTD, simulation is performed in the three segments separately and detail of which is described in available literature [17].

2.4. Hybrid FDTD Method

Hybrid FDTD method is developed by combining Friis transmission equation with FDTD method. In this method, EM modelling of the simulating elements is prepared using conventional FDTD method and power calculation of the plane wave source required for the simulation is made by Friis transmission formula [18]:

$$\frac{P_r}{P_t} = \frac{G_t A_{er}}{4\pi R^2} \tag{1}$$

where, P_r = received power (W), P_t = transmitted power (W), G_t = gain of the transmitting antenna, A_{er} = effective aperture of receiving antenna (m^2) and R = distance from the antenna (m).

After a distance in the order of tens of wavelengths, the field from most antennas behaves like a plane wave [19]. For that reason the simulation model as shown in Fig. 1 is divided into two sub domains namely domain 1 and 2 as shown in Fig. 3. Domain 1 is used to compute the characteristics of resultant fictitious plane wave source. This plane wave source is actually a replacement of the radiating BSA placed at a distance R from the human model and its properties are calculated from Equation (1) considering transmitted power $P_t = 20\,\mathrm{W/carrier}$, detail of which is described in available literature [20]. In domain 2, the fictitious plane wave is placed at a distance of $r = 25\,\mathrm{mm}$ away from the human model and the desired parameters are calculated.

The amplitude of the E field intensity at a distance R from the antenna can be calculated with the following equation [20]:

$$E_0 = \sqrt{\eta_0 \frac{P_r}{A_{er}}} = \frac{1}{R}\sqrt{120\pi \frac{P_t G_t}{4\pi}} = \frac{\sqrt{30 P_t G_t}}{R} \tag{2}$$

Similarly, magnitude of H field intensity can also be calculated by the following equation [4]:

$$H_0 = \frac{E_0}{\eta_0} \tag{3}$$

where, $\eta_0 = 120\pi\,\Omega = 377\,\Omega$.

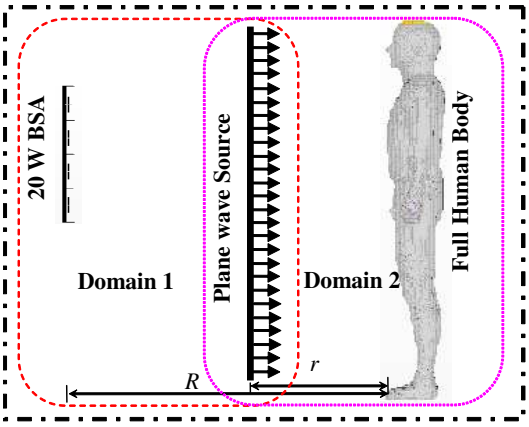

Figure 3. Geometry of human model along with BSA [$R = 0.5\,\text{m}$ to $1.5\,\text{m}$ and $r = 25\,\text{mm}$].

2.5. SAR Calculation

From the converged solutions, the local SAR at (i, j, k)th cell inside the whole body is obtained from the following equation [4]:

$$\text{SAR} = \frac{\sigma\,|E^2|}{2\rho}\ (\text{W/kg}) \tag{4}$$

where, E is the electric field (V/m), σ = conductivity of the head (S/m) and ρ = mass density of the body tissues (kg/m^3).

3. RESULTS AND DISCUSSION

Variations of S_{11} in dB and gain in dBi with frequency for a single dipole antenna and the BSA computed using conventional FDTD method by MATLAB and CST Microwave Studio® respectively are shown in Figs. 4–5. From Fig. 4, it is found that at the fundamental mode, the single dipole antenna and BSA resonate at 928.9 MHz and 925.0 MHz with S_{11} value of $-42.00\,\text{dB}$ and $-41.75\,\text{dB}$ respectively. Value of S_{11} is below $-20\,\text{dB}$ within GSM 900 band. From Fig. 5, it is found that maximum values of the gain are equal to 1.67 dBi and 6.37 dBi at 1000 MHz for the single dipole antenna and the BSA consists of cavity backed dipole array. At 925 MHz 5.75 dBi gain has been achieved for this BSA.

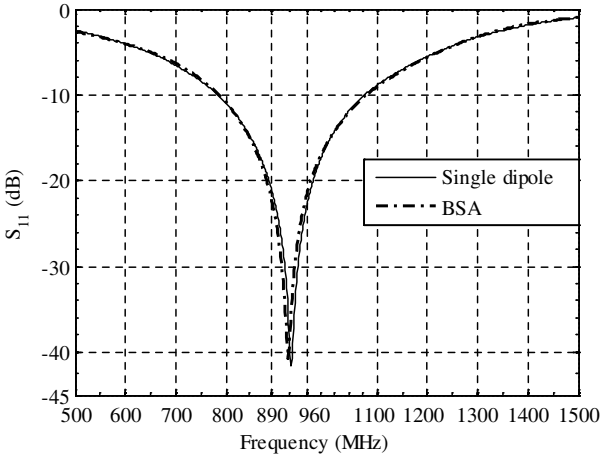

Figure 4. S_{11} vs. Frequency of single dipole antenna and BSA.

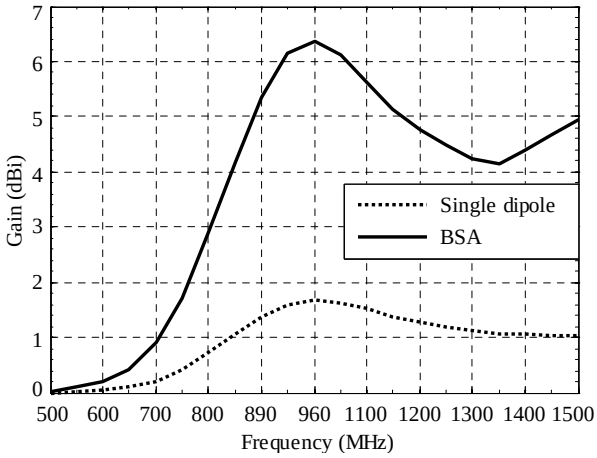

Figure 5. Gain vs. Frequency of single dipole antenna and BSA.

The distributions of E and H field intensities in free space for distance up to 5.0 m have been computed using CST Microwave Studio®. Distributions of E field and H field intensity at 925 MHz in the mid YZ-plane and XY-plane for BSA are shown in Figs. 6–7. Peak value of E and H field intensity at 5.0 m away from the BSA antenna are found to be 24.1 V/m and 0.06 A/m respectively. The peak value of E and H field at 5.0 m away from the BSA can also be calculated using the Equations (2) and (3), and becomes approximately equal to 23.5 V/m and 0.06 A/m which closely agrees with the value obtained using CST Microwave Studio®.

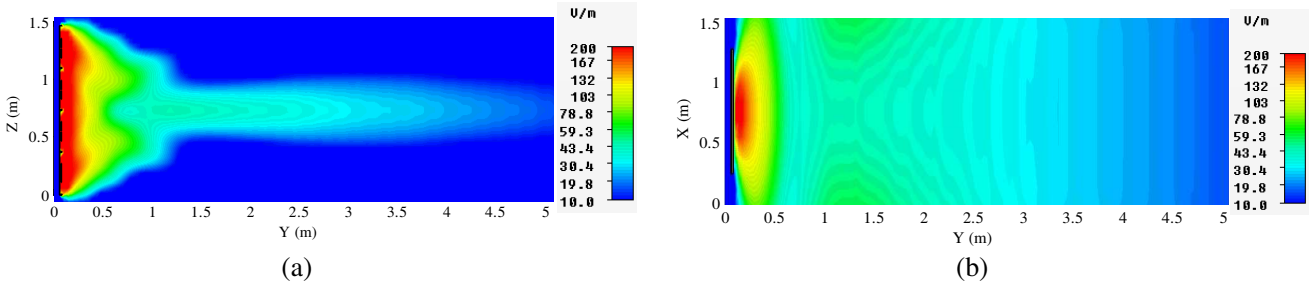

Figure 6. E field distributions at 925 MHz in (a) YZ-plane and (b) XY-plane in free space.

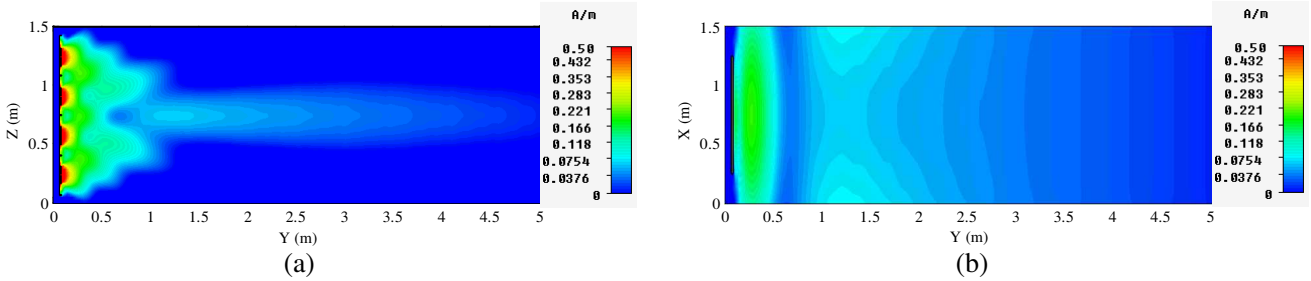

Figure 7. H field distributions at 925 MHz in (a) YZ-plane and (b) XY-plane in free space.

In India, the GSM 900 base station antenna transmits in the frequency range of 935 MHz–960 MHz (base station to handset) providing 124 RF channels (channel numbers 1 to 124) spaced at 200 kHz. The method chosen by GSM is a combination of Time-and Frequency-Division Multiple Access (TDMA/FDMA). The FDMA part involves the division by frequency of (maximum) 25 MHz bandwidth which is divided into twenty sub-bands of 1.2 MHz and is allocated to various operators. There may be several number of carrier frequencies (1 to 5) allotted to one operator with upper limit of 6.2 MHz bandwidth. Each carrier frequency may transmit 10 to 20 W of power. So, one operator may transmit 50 to 100 W of power. There may be 3–4 operators on the same roof top or tower; therefore, total transmitted power may be 200 to 400 W.

Time and frequency domain GSM 900 band downlink spectrum for five carrier frequencies are shown in Figs. 8(a)–(b). The spikes as shown in Fig. 8(b) are corresponding to the frequencies (carriers) used by the operator.

SAR distributions in dB scale inside the human body model at the mid-saggital and mid-coronal planes for $R = 0.5$ m due to five carrier are shown in Figs. 9(a)–(b). From Fig. 9, it is seen that higher value of SAR is found in the superficial region of the human body model consisting of mainly skin tissue. But lower value of SAR is induced in thoracic and abdominal cavity region of the human body model, major portion of which is filled with air.

Variations of $\mathrm{SAR_{WB}}$ with R for multiple numbers of carrier frequencies obtained by hybrid FDTD and SFDTD method are shown in the Fig. 10. From Fig. 10, it is found that $\mathrm{SAR_{WB}}$ obtained by hybrid FDTD method closely matches with that obtained by the SFDTD method. Either due to increase of R or decrease the number of carrier frequencies, $\mathrm{SAR_{WB}}$ decreases. For number of carrier frequency equal to five and $R = 0.5$ m, maximum value of $\mathrm{SAR_{WB}}$ obtained by both hybrid FDTD and SFDTD

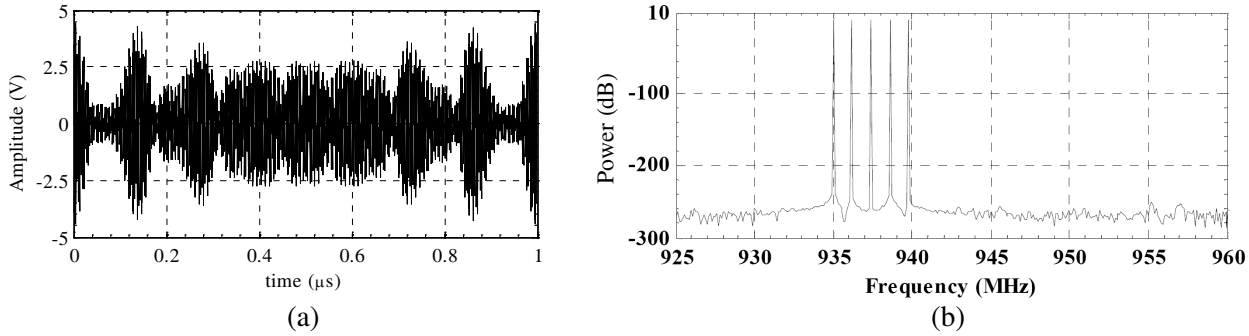

Figure 8. Spectrum of 5 carrier frequencies in (a) time domain and (b) frequency domain.

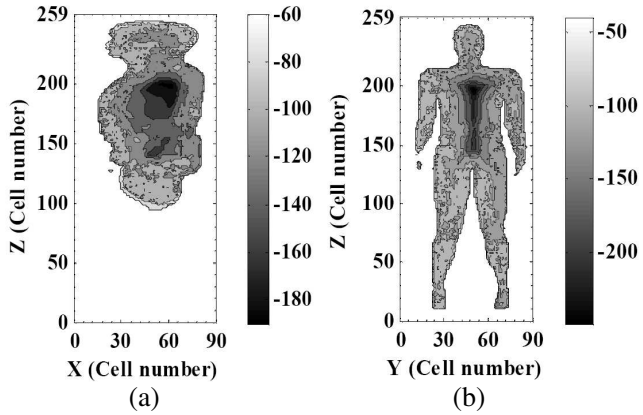

Figure 9. SAR distributions in (a) mid-saggital plane and (b) midcoronal plane for $R = 0.5\,\mathrm{m}$ and five carrier frequencies.

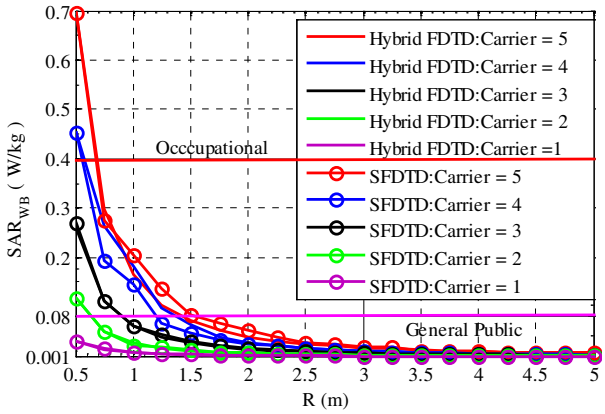

Figure 10. Variations of $\mathrm{SAR_{WB}}$ with R for multiple numbers of carrier frequencies.

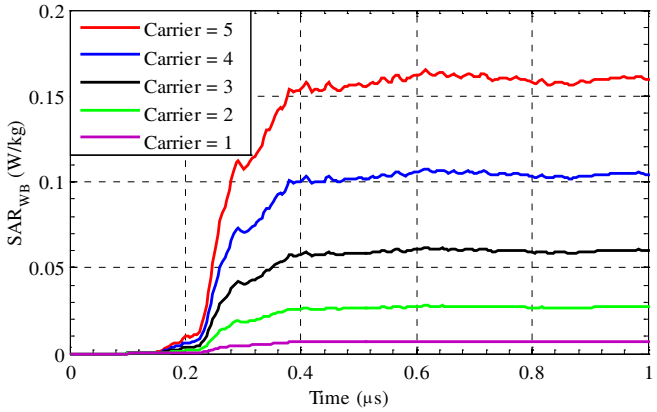

Figure 11. Variations of $\mathrm{SAR_{WB}}$ with Time obtained by hybrid FDTD method for multiple numbers of carrier frequencies and $R = 1.0\,\mathrm{m}$.

method is found to be 0.69 W/kg which exceeds the occupational exposure safety limit but for R more than 1.5 m, value of $\mathrm{SAR_{WB}}$ is below the general public exposure safety limit. From the simulation it is found that the value of safety distance for general public is 1.5 m due to five number of carrier frequencies but it's value decreases with lowering the number of carrier frequencies.

Variations of $\mathrm{SAR_{WB}}$ with Time for multiple numbers of carrier frequencies and $R = 1.0\,\mathrm{m}$ obtained

by hybrid FDTD method are shown in Fig. 11. From Fig. 11, it is found that after 0.2 μs settling time, with increase of time SAR_{WB} increases exponentially for very short period of time then it becomes almost constant for each number of carrier frequencies. Steady-state value of SAR_{WB} increases with increase of number of carrier frequencies and vice-versa.

In SFDTD method, simulation domain corresponding to the antenna segment, intermediate segment and body segment consists of $117 \times 117 \times 272$ Yee cells, $70 \times 70 \times 231$ Yee cells and $91 \times 94 \times 261$ Yee cells respectively. But the simulation domain used in hybrid FDTD method consists of $91 \times 96 \times 261$ Yee cells. Therefore, it is seen that the total size of the simulation domain used in SFDTD method is larger than that used in the hybrid FDTD method. Summary of performance comparison of SFDTD method with hybrid FDTD method in terms of computational time and memory usage for the MATLAB programs run in a PC consists of Intel Pentium Dual CPU T2330 @ 1.60 GHz and 4 GB RAM is shown in Table 1. From the table it is seen that hybrid FDTD method is faster and requires less memory than SFDTD method.

Table 1. Performance comparison of SFDTD method with hybrid FDTD method.

Method	Memory usage (MB)	Computational time (s)
SFDTD	2859	65746.07
Hybrid FDTD	948	18784.59

4. CONCLUSION

SAR_{WB} induced within a realistic full human body model based on CT scan data exposed to a BSA at GSM 900 band for R in the range of 0.5 m to 5.0 m has been calculated using hybrid FDTD method and compared that with the results obtained by SFDTD method for multiple number of carrier frequencies. Transmitted power from BSA is equal to 20 W/carrier. In order to investigate the behavior of the EM field in the vicinity of the BSA distance up to 5.0 m, the distributions of the E and H field intensities in free space have been computed using CST Microwave Studio®. Value of safety distance for general public from the BSA is found to be 1.5 m due to number of carrier frequencies equal to five, but this value decreases with lowering the number of carrier frequencies.

The hybrid FDTD consists of Friis transmission equation and FDTD method. Compared to SFDTD method, hybrid FDTD method drastically reduces the computational complexity resulting in less memory usage and faster execution.

REFERENCES

1. Kundi, M. and H. P. Hutter, "Mobile phone base stations-effects on wellbeing and health," *Pathophysiology*, Vol. 16, 123–135, ELSEVIER, Aug. 2009.
2. Stalling, W., *Wireless Communication and Networks*, Prentice Hall, 2002.
3. Kumar, N. and G. Kumar, "Biological effects of cell tower radiation on human body," *International Symposium on Microwave and Optical Technology (ISMOT)*, Dec. 2009, Available: http://briarcliffheights.org/bch/wp-content/uploads/2011/12/celltowerradiationeffects-100317162351-phpapp01.pdf.
4. Ali, F., R. R. Sahoo, and S. Ray, "Study of maximum local temperature rise and hotspots distribution in a human head for GSM900 mobile phone," *International Conference on Eco-friendly Computing and Communication Systems (ICECCS)*, 72–78, Advances in Energy Aware Computing and Communication System, Tata McGraw Hill, India, Oct. 2013, ISBN-13:978-9-35-13432-5.
5. Lennart, H., "Epidemiological evidence for an association between use of wireless phones and tumor diseases," *Pathophysiology*, PATPHY-595, ELSEVIER, 2009.
6. Blackman, C. F., et al., "Effects of ELF fields on calciumion efflux from brain tissue in vitro," *Radiation Research*, Vol. 92, 510–520, 1982.

7. Lai, H. and N. P. Singh, "Melatonin and a spin-trap compound block radiofrequency electromagnetic radiation-induced DNA strand breaks in rat brain cells," *Bioelectromagnetics*, Vol. 18, 446–454, 1997.
8. Kundi, M. and H. Peter, "Mobile phone base stations-effect on wellbeing and health," *Pathophysiology*, Vol. 16, 123–135, ELSEVIER, 2009.
9. ICNIRP, "Guidelines for limiting exposure to time- varying electric, magnetic, and electromagnetic fields (10 kHz to 300 GHz)," *Health Physics*, Vol. 74, No. 4, 494–522, Apr. 1998.
10. Council of the European Communities, "Recommendation of 12 July 1999 on the limitation of exposure of general public to electromagnetic fields (0 Hz to 300 GHz)," *Official Journal of the European Communities*, L.199/59-61, Jul. 30, 1999.
11. Karwowski, A., "Evaluating exposure to radio-frequency emissions from base station antennas," *13th IEEE International Symposium on Personal, Indoor and Mobile Radio Communications (PIMRC)*, 1877–1881, Dec. 2002, Available: http://ieeexplore.ieee.org/xpl/login.jsp?tp=&arnumber=1045504&url=http%3A%2F%2Fieeexplore.ieee.org%2Fxpls%2Fabs_all.jsp%3Farnumber%3D1045504.
12. Karwowski, A., "Comparison of simple models for predicting radiofrequency fields in vicinity of base station antennas," *Electronics Letters*, Vol. 36, No. 10, 859–861, May 2000.
13. Wu, Y. and I. Wassell, "Introduction to the segmented finite-difference time-domain method," *IEEE Trans. on Magnetics*, Vol. 45, No. 3, 1364–1367, Mar. 2009.
14. MATLAB 7.1, The MathWorks, Inc., Available: http://www.mathworks.com.
15. The Zubal Phantom data, MRI Head Phantom Data Description, Available: http://noodle.med.yale.edu/phantom//tissman/ArmsDownTiss3-6/vox_tiss8.dat.
16. "Dielectric properties of the human body tissue in the frequency range of 10 Hz–100 GHz," Available: http://niremf.ifac.cnr.it/tissprop.
17. Ali, F. and S. Ray, "SAR analysis using SFDTD and hybrid FDTD," *5th International Conference on Computers and Devices for Communication (CODEC) MMT*, 1–4, Institute of Radio Physics and Electronics, University of Calcutta, India, Dec. 2012.
18. Kraus, J. D. and R. J. Marhefka, *Antennas for All Applications*, Tata Mc.Graw-Hill Publishing Company Limited, New Delhi, India, Third Reprint, 2003.
19. Sullivan, D. M., *Electromagnetic Simulation Using the FDTD Method*, IEEE Press, New York, 2000.
20. Ali, M. F. and S. Ray, "Study of EM wave absorption and shielding characteristics for a bonsai tree for GSM-900 band," *Progress In Electromagnetics Research C*, Vol. 49, 149–157, 2014.